

# Thrust Vector Control Utilizing Asymmetric Jet Nozzles

Gustave J. Hokenson\*

The Hokenson Company, Los Angeles, California

RECENTLY interest in thrust vector control with rigidly mounted thrusters has been revived. The results described in this Note are associated with the side-force generated by a supersonic jet with an exit plane which is oblique to the centerline of the exhaust flow. As shown in Fig. 1, depending on whether the flow is over- or under-expanded, the direction of the exhaust flow is deflected either toward or away from the normal to the exit plane by an amount related to the pressure imbalance and the projected area of the exit plane in the lateral direction.<sup>1</sup> Therefore, control over the direction and amount of side-force is available by varying the stagnation pressure and exit plane obliquity.

Although the present results are associated with a two-dimensional configuration, with the exit plane obliquity established by extending one wall of the nozzle, application to an axisymmetric configuration is conceivable. For example, consider a fixed axisymmetric thruster enclosed by a cylindrical housing which is split longitudinally into various sections (see Fig. 1). At the null position, the end of the cylinder coincides with the exit plane of the thruster. As various combinations of cylindrical sections are translated forward of the exit plane, the radially projected area of the exit plane may be oriented toward any azimuthal angle. The amount of projected area and its orientation may also be changed rapidly, which adds another control feature to the thrust vectoring.

The focus of the work described in Ref. 2 involved the extent to which viscous effects affected the performance, particularly at over-expanded conditions. A two-dimensional supersonic jet of aspect ratio (height/width) equal to 1.5 was established over the Mach number range 1.0 to 3.0. One wall of the nozzle contour was then extended a specified fraction of the nozzle contour to establish an oblique exit plane. Transparent and parallel lateral sidewalls bounded the nozzle and extensions thereof through which the flow angle could be observed. The side force generated was measured with a strain gage balance to an accuracy of  $\pm 2\%$  of the reading, based on the scatter in repeated experiments and comparison to the measured flow angle.

In order to assess the degree to which viscous effects impede accurate analytical prediction, the amount of asymmetry was limited to maintain the wall extension within the domain established by the Mach wave originating from the opposite nozzle wall at the exit plane.

Figures 2-4 depict the forces measured on three nozzles whose exit plane is offset by an amount 1.0, 4/3, and 5/3 times the jet height, respectively. Comparison with predictions of two-dimensional inviscid flow theory is shown also. These results may be converted into force coefficients by dividing the results by the surface area of the wall extension and the exit dynamic pressure. The corresponding plot of the Fig. 3 data is presented in Fig. 5. These results indicate that, even in the simple case established here, nontrivial deviations between inviscid flow theory and experiment are observed, although the general trends predicted by analysis are correct. It is also clear that the vectoring control may extend well into the over-expanded region before the nozzle boundary layers begin to

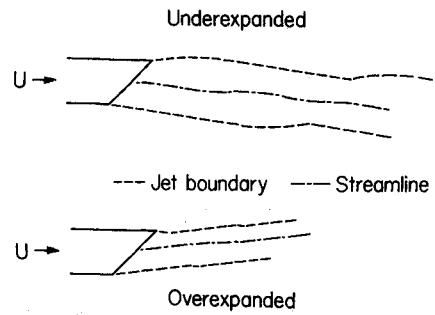


Fig. 1 Configuration of the nozzle, jet boundary, and center streamline for two-dimensional (and a longitudinal slice of an azimuthally varying axisymmetric nozzle) flow in under- and over-expanded conditions.

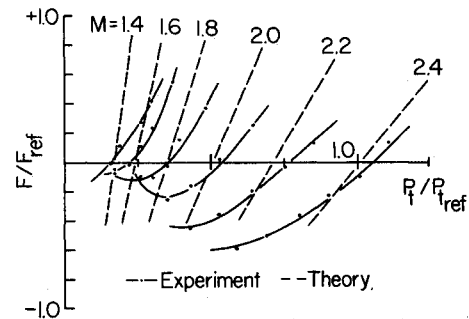


Fig. 2 Side-force vs stagnation pressure for various Mach numbers on a two-dimensional supersonic jet nozzle with an asymmetric exit plane. Asymmetry factor (nozzle wall extension/nozzle exit height) = 1.0,  $F_{ref} = 0.5$  lb,  $P_{tref} = 200$  psig.

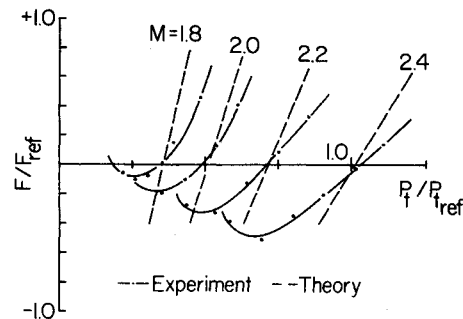


Fig. 3 Side-force vs stagnation pressure for various Mach numbers on a two-dimensional supersonic jet nozzle with an asymmetric exit plane. Asymmetry factor (nozzle wall extension/nozzle exit height) = 4/3,  $F_{ref} = 0.5$  lb,  $P_{tref} = 200$  psig.

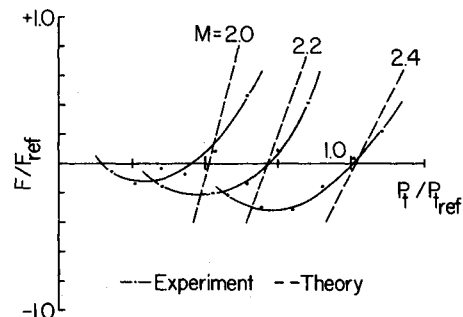


Fig. 4 Side-force vs stagnation pressure for various Mach numbers on a two-dimensional supersonic jet nozzle with an asymmetric exit plane. Asymmetry factor (nozzle wall extension/nozzle exit height) = 5/3,  $F_{ref} = 0.5$  lb,  $P_{tref} = 200$  psig.

Received Sept. 16, 1985; revision received Nov. 18, 1985. Copyright © American Institute of Aeronautics and Astronautics, Inc., 1986. All rights reserved.

\*Chief Scientist. Member AIAA.

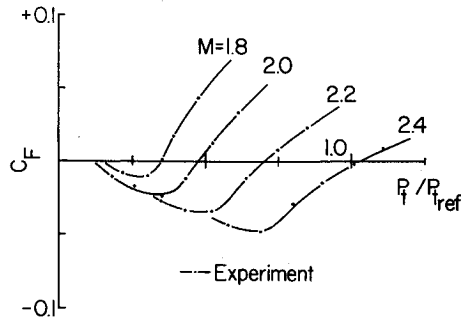


Fig. 5 Side-force coefficient vs stagnation pressure for various Mach numbers for the data from Fig. 2. Reference area and pressure are the lateral projected area of the asymmetry and the exit dynamic pressure.

separate and the entire flow degrades, although the Reynolds number dependence of the effect in this configuration remains to be quantified. On the basis of these data, it is concluded that control of the thruster plenum pressure and exit plane obliquity (including the aforementioned axisymmetric case wherein the sideforce vector may be oriented azimuthally) provides the ability to quickly orient the thrust vector of nongimbal-jets.

#### Acknowledgments

The data in Ref. 2 were acquired while the author was on the faculty of the Department of Aeronautics at the U.S. Naval Postgraduate School. Preparation of this paper was supported by the Aerospace Sciences Directorate of AFOSR and the Office of Basic Energy Sciences, Department of Energy.

#### References

- <sup>1</sup>Ferri, A., *Elements of Aerodynamics of Supersonic Flows*, The Macmillan Company, 1949, pp. 170-172.
- <sup>2</sup>Horais, Brian J., "Vectored Thrust Control," MS Thesis, U.S. Naval Postgraduate School, Monterey, CA, Dec. 1972.

## $\vec{v} \times \vec{B}$ and Density Gradient Electric Fields Measured from Spacecraft

J.R. Lilley Jr.,\* I. Katz,† and D.L. Cooke\*  
S-Cubed, LaJolla, California

#### Nomenclature

$e$	= electron charge
$\ell$	= distance
$\vec{v}$	= velocity of satellite
$\vec{B}$	= magnetic field
$\vec{E}$	= electric field
$L$	= approximate radius of spacecraft
$\vec{F}_L$	= Lorentz force
$n_i, n_e$	= ion, electron density
$n_1, n_2$	= local ion densities in spacecraft wake
$n_0$	= undisturbed electron density

Received June 24, 1985; revision received Nov. 5, 1985. Copyright © American Institute of Aeronautics and Astronautics, Inc., 1986. All rights reserved.

\*Research Scientist.

†Program Manager. Member AIAA.

$\phi$  = local potential  
 $\theta_e$  = electron temperature, V

THE electric fields observed on satellites can be due to a number of environmental influences. Density gradients and  $\vec{v} \times \vec{B}$  are two causes of electric fields measured in low earth orbit. The electric fields due to density gradients mainly affect the smaller satellites, while voltages generated by moving through magnetic fields are dominant on larger objects. For spacecraft the size of the Space Shuttle Orbiter (10-30 m), the two effects are of the same order of magnitude. Measurements made during flights of the orbiter support this observation.

When a good conductor moves magnetic field lines, it develops a tangential electric field to cancel the Lorentz force on its conduction electrons. The tangential electric field can be found in the plasma's frame of reference by solving

$$\vec{F}_L = e(\vec{E} + \vec{v} \times \vec{B}) = 0$$

to find

$$\vec{E} = -\vec{v} \times \vec{B} \quad (1)$$

An electric field is also generated by the density gradient found in the wake of a fast-moving spacecraft through a dense plasma. By fast, we mean that the spacecraft is supersonic with respect to the dominant ion species, and by dense, we mean that spacecraft dimensions are large compared with the unperturbed ionospheric plasma Debye length. The Shuttle Orbiter satisfies both these conditions. The potential in the wake can be estimated using quasineutrality and the Boltzmann relation for electrons.

$$n_i \approx n_e$$

$$n_e = n_0 e^{(\phi/\theta_e)}$$

Solving for  $\phi$

$$\phi = \theta_e \ln(n_e/n_0)$$

the electric field resulting from density gradients can be approximated by the change in the local potential over a length roughly the size of the cross-section of spacecraft with respect to the ram direction. Or

$$\vec{E} \approx -(\Delta\phi/L) \approx -(\phi/L)[\ln(n_2/n_0) - \ln(n_1/n_0)] \quad (2)$$

The magnitude of electric fields due to the two effects can be approximated using Eqs. (1) and (2). Assuming a  $10^{11} \text{ m}^{-3}$  plasma with a magnetic field of 0.4 G and a density gradient of four orders of magnitude in the wake (as observed on the Shuttle Orbiter) at low altitudes and higher latitudes, we can estimate the magnitude of the electric fields caused by both processes. Using an orbital velocity of 7.7 km/s, the  $\vec{v} \times \vec{B}$  field would be 0.31 V/m and independent of vehicle dimensions. Table 1 is for density gradient fields and, as can be seen from Eq. (2), depends inversely on the size of the orbiting spacecraft.

The electric field magnitudes lead one to expect small satellites ( $\sim 1-2$  m in diam) to have local fields dominated by density gradient fields and large spacecraft ( $\sim 50-200$  m, i.e.,

Table 1 Electric fields due to density gradients of four orders of magnitude<sup>1</sup>

$L, \text{ m}$	$\theta = 0.1 \text{ eV}$	$\theta = 0.2 \text{ eV}$
	$E, \text{ V/m}$	$E, \text{ V/m}$
0.5	1.8	3.7
5.0	0.18	0.37
50.0	0.018	0.037